Title
ALPHA DECAY OF SPHEROIDAL NUCLEI

Authors
Rasmussen, John O.
Segall, Benjamin.

Publication Date
1955-10-07

UCRL 3040

UNIVERSITY OF CALIFORNIA

Radiation Laboratory

BERKELEY, CALIFORNIA

DISCLAIMER

UCRL-3040

UNIVERSITY OF CALIFORNIA
Radiation Laboratory
Berkeley, California

Contract No. W-7405-eng-48

ALPHA DECAY OF SPHEROIDAL NUCLEI

John O. Rasmussen
and
Benjamin Segall

October 7, 1955

Printed for the U. S. Atomic Energy Commission

Alpha Decay of Spheroidal Nuclei

John O. Rasmussen
Radiation Laboratory and Department of Chemistry
University of California, Berkeley, California

and

Benjamin Segall*
Radiation Laboratory
University of California, Berkeley, California

October 7, 1955

ABSTRACT

The consequences of spheroidal deformation of nuclei on the barrier transmission in alpha decay are considered. A set of coupled differential equations is derived relating the amplitudes of the various groups of alpha particles emitted from a nucleus described by the Bohr-Mottelson model. The cases of the decay of Th^{228} and Cm^{242} were studied numerically and from them information regarding the probability distribution of alpha particles on the nuclear spheroidal surface is obtained. It is found that the one-body model of an alpha particle in a well does not yield these distributions, and it is thus concluded that "alpha-particle clusters" have a short mean-free path in nuclear matter. The shift in the surface distributions of Th^{228} and Cm^{242} may be explained qualitatively in terms of the order of nucleon orbital filling.

The overall penetration factors for the spheroidal case are compared with those for the spherical case and the resultant enhancement due to the deformation is not nearly as large as that predicted by Hill and Wheeler on the basis of a one-dimensional approximation.

---

*Present address: General Electric Research Laboratory, Schenectady, N. Y.

Alpha Decay of Spheroidal Nuclei

John O. Rasmussen
Radiation Laboratory and Department of Chemistry
University of California, Berkeley, California

and

Benjamin Segall*
Radiation Laboratory
University of California, Berkeley, California

October 7, 1955

INTRODUCTION

Recently an impressive amount of data have been amassed demonstrating the existence of rotational spectra in regions far removed from closed-shell configurations.[1] The existence of such level schemes is predicted by the Bohr-Mottelson[2] strong-coupling model of the nucleus in which it is assumed that the nucleus has an appreciable spheroidal deformation.

In the region of heavy nuclei ($A \gtrsim 230$) where alpha decay is generally a prominent mode of decay the rotational bands are particularly well developed, and some cases of alpha emission by even-even nuclei to members of the rotational band as high as the 8+ level have been observed.[3] Alpha decay of even-even nuclei to states other than the rotational band members has been observed only in the case of a few nuclides.

One of the most conspicuous features of the recent data involves the variation between nuclei of the relative intensities of the various alpha groups. Asaro[4] has calculated "hindrance" factors for all alpha groups, where the hindrance factor is defined as the ratio of the intensity of the alpha group leading

---

*Present address: General Electric Research Laboratory, Schenectady, N. Y.

to the ground state to the intensity of the alpha particles leading to the particular excited state, corrected for the energy difference between the states. For the energy dependence of the decay rate he used Preston's[5] alpha-decay formula (for no spin change[6]). Figure 1, which is due to Asaro, summarizes the data.

It is to be expected that the occurrence of large spheroidal deformations will have pronounced effects on the process of charged-particle emission. In contrast to the case of spherical nuclei the electrostatic field of a spheroid is not central. The coupling resulting from the non-central nature of the field will have a bearing on the relative amplitudes of particles emitted with different orbital angular momenta. It is one of the purposes of this note to see whether it is possible to explain the values and trends for the hindrance factors of the $L = 2$ and $L = 4$ waves in the decay of even-even nuclei in terms of the non-central electrostatic field.

Another consequence of the distortion of the nucleus, earlier explored by Hill and Wheeler,[7] is a thinning out of the potential barrier in certain directions leading to directed alpha emission in those directions. They gave an approximate expression for the penetrability based on a one-dimensional WKB integration through the "thinnest" part of the barrier. It is to be noted though that if the decay is highly directional with respect to the nuclear symmetry axis, it is necessary that components of the alpha waves with high L values[8] occur with large amplitudes. These would be the components leading to the higher rotational states. Since these components experience a much larger effective potential than the S-wave due to the centrifugal potential and the additional energy associated with rotation of the recoil nucleus, one might expect significant deviations from the penetration formula of Hill and Wheeler[7] based on a one-dimensional WKB integration through the thinnest part of the

barrier. In the final section of this note are calculated the total barrier penetrabilities for Cm^{242} and Th^{228}.

In the next section we derive the general equations governing alpha decay to a rotational band of the daughter nucleus. In the section following this equations for decay from an even-even nucleus are formulated in prolate spheroidal coordinates, and these equations serve as the basis for the subsequent exploratory numerical work.

FORMULATION OF THE ALPHA-DECAY PROCESS

To formulate the problem of alpha decay in the region external to the nuclear surface it is necessary to take into account the electrostatic interaction between the alpha particle and the residual nucleus. The first question to be settled is which degrees of freedom of the nucleus are required for an appropriate description of the process. In the case of a spherical daughter nucleus it is easy to see that it is unnecessary to consider the Coulomb interaction between the alpha particle and the protons individually as this force is very much smaller than nuclear forces. It thus suffices to consider only the interaction of the alpha particle with the nucleus as a whole, and the appropriate nuclear coordinates are those of the center of mass of the system. In the case of a deformed nucleus the interaction between the alpha particle and the quadrupole field of the nucleus is not small compared to the energy characterizing rotation. Here it is necessary to include in the description of the process the rotational coordinates of the nucleus. Expressing it alternatively, it is necessary to include in the total wave function the low-lying rotational states. The emitted alpha particle can then be thought to induce transitions between the rotational states through the quadrupole component of the field.

In general the Schrödinger equation for the system can be reduced to a system of coupled equations in the variable r by expanding the wave function in terms of some complete orthogonal set of functions in the remaining variables:

$$\Psi = \sum_{\gamma} R_{\gamma}(r)\Omega_{\gamma}(x_i, \theta, \phi) \qquad (1)$$

where x_i is the set of variables required to describe the recoil nucleus.

Multiplication by Ω^*_{γ} and integration over all variables except r reduces the partial differential equation to a set of ordinary differential equations in r (cf. Preston[9]). Ω_{γ} can be expanded in terms of products of eigenfunctions of the residual nucleus and normalized spherical harmonics $Y_{\ell, m}(\theta, \phi)$ in the angles of the alpha particle with respect to axes fixed in space. The set necessary to describe the decay process is limited by the constraints that the angular momentum of the parent nucleus I_i and its space projection M_i be conserved. The constraints are satisfied by the summation[10]

$$\Phi^{I_i\ M_i}_{I_f\ \ell} = \sum_{m} (I_f\ \ell\ m\ M_i\text{-}m \,|\, I_f\ \ell\ I_i\ M_i)\ \chi^{\tau}_{I_f\ M_i\text{-}m}(x_i) Y_{\ell, m}(\theta, \phi) \qquad (2)$$

where $(I_f\ \ell\ m\ M_i\text{-}m\,|\,I_f\ \ell\ I_i\ M_i)$ are the Clebsch-Gordan coefficients, and $\chi^{\tau}_{I_f\ M_i\text{-}m}(x_i)$ is a normalized nuclear wave function for a state with angular momentum I_f, component M_f, and with remaining quantum numbers τ.

The set of equations obtained from (1) and (2) will contain coupling terms the strength of which will depend on the magnitude of the electric transition moments connecting the nuclear states involved. The outstanding examples of large electric moments between nuclear states are those resulting in the "fast" electric quadrupole transitions between members of a rotational band. Thus, we see that the low rotational bands, both because their members constitute the low-lying nuclear states and because band members are connected by

large matrix elements, are the appropriate nuclear states for our problem. We shall in the following restrict ourselves to the decay to the states of one band.

For explicit nuclear wave functions we turn to the recent work of Bohr and Mottelson[1] in which nuclear motion is approximately separated into "rotational" and "intrinsic" parts. In the Bohr-Mottelson model of strongly deformed nuclei the rapid individual particle motion is thought to take place in a deformed nuclear field (or well) which rotates nearly adiabatically. The deformed nuclear field is taken to have axial symmetry, although there may be cases where this is not true.[11] The wave function for the nucleus then approximately factors (apart from a symmetrization) into

$$\chi^{\tau}_{I_f M_f K_f} = \varphi_{\tau}(x_i') \, D^{I_f}_{M_f K_f}(\Theta_i) \cdot \left(\frac{2I_f+1}{8\pi^2}\right)^{1/2} \tag{3}$$

where $\varphi_{\tau}(\vec{x}_i')$ is the state of the particle structure, $\vec{x}_i'$ being the coordinates of particles with respect to a frame of reference fixed in the nucleus, and $\left(\frac{2I_f+1}{8\pi^2}\right)^{1/2} D^{I_f}_{M_f K_f}(\Theta_i)$ is the normalized state of rotation (or wave function for a symmetrical top) having as arguments the Eulerian angles $(\Theta)_i$. K_f denotes the projection of the angular momentum of nucleus, I_f, on the symmetry axis, and is in this model an approximate constant of the motion. τ represents all the quantum numbers specifying the intrinsic state. The Hamiltonian of which (3) is an eigenfunction is

$$H_{nucl.} = H_p(x_i') + H_{ROT}(\Theta_i) \tag{4}$$

where $H_p(\vec{x}_i')$ is the energy operator for the individual particles in the deformed well and $H_{rot.}(\Theta)$ is the rotational energy operator which gives rise to a spectrum of the form

$$E_I = (\hbar^2/2\mathfrak{I})I(I+1)$$

$\mathfrak{I}$ is interpreted as a moment of inertia and is for the irrotational fluid approximation proportional to the square of the deformation.

To obtain the complete Hamiltonian for the alpha decay problem in the center of mass system we add to (4) the energy operator for the alpha particle in the region outside the short range nuclear force field:

$$H_a = (\hbar^2/2\mu)\Delta + V_{el.}(\vec{r}\,;\Theta_i) \,. \tag{5}$$

The inclusion of Θ_i in the electrostatic energy indicates that the field at a point in the space-fixed system varies as the daughter nucleus rotates. μ is the reduced mass of the system.

A consequence of the assumption that the nuclear well is axially symmetric is that the nucleons within the nucleus have an axially symmetric distribution. This will reflect itself in a corresponding symmetry for the alpha particles on the surface. To incorporate this symmetry into our formulation of the problem and also to effect a simplification of the electrostatic interaction we shall consider the description of the process in a system of coordinates fixed in the daughter nucleus, i.e., with the nuclear symmetry axis taken to be the polar axis. We then expand the wave function of the system as

$$\Psi = \sum_{\ell, m} r^{-1} \, w_{\ell, m}(r) \, \Upsilon^{I_i M_i}_{K_f \ell m; \tau} \tag{6}$$

where $w_{\ell, m} \to e^{ikr}$ when $r \to \infty$

$$\Upsilon^{I_i M_i}_{K_f \ell m; \tau} = \varphi_\tau(x_i') \left(\frac{2I_i+1}{8\pi^2}\right)^{\frac{1}{2}} D^{I_i}_{M_i; K_f+m}(\Theta_i) \, Y_{\ell, m}(\theta', \varphi') \tag{7}$$

and (r, θ', ϕ') are the spherical polar coordinates in the new system.

That (7) has the proper transformation properties (i.e., represents a state with angular momentum I_i and component M_i) and contains the rotational states of the daughter nucleus can be demonstrated by transforming to space-fixed coordinates (r, θ, ϕ). For this purpose, we make use of the transformation properties of the spherical harmonics

$$Y_{l,m}(\theta',\varphi') = \sum_{m'} D^{l}_{m'm}(\Theta_i)\, Y_{l,m'}(\theta,\varphi) = \sum_{m'} (-)^{m'+m} D^{l}_{-m'-m}(\Theta_i)\, Y_{l,m'}(\theta,\varphi) \tag{8}$$

and the Clebsch-Gordan expansion for the D's

$$D^{l}_{-m',-m}(\Theta_i)\, D^{I_i}_{M_i,K_f+m}(\Theta_i) = \sum_{I_f=|I_i-l|}^{I_i+l} (I_i\, l\, M_i - m' | I_i\, l\, I_f\, M_i - m')(I_i\, l\, K_f + m - m | I_i\, l\, I_f\, K_f) \times D^{I_f}_{M_i-m',K_f}(\Theta_i) \tag{9}$$

to obtain

$$\begin{aligned}
\Upsilon^{I_i M_i}_{K_f l\, m;\tau} &= \varphi_\tau(x') \left(\frac{2I_i+1}{8\pi^2}\right)^{\frac{1}{2}} \sum_{I_f} (-)^{m} (I_i\, l\, K_f+m\, -m | I_i\, l\, I_f\, K_f) \\
&\quad \times \sum_{m'} (-)^{m'} (I_i\, l\, M_i - m' | I_i\, l\, I_f\, M_i - m')\, D^{I_f}_{M_i-m',K_f}(\Theta_i)\, Y_{l,m'}(\theta,\varphi) \\
&= \varphi_\tau(x') \sum_{I_f} (-)^{m+I_f-I_i} (I_i\, l\, K_f+m\, -m | I_i\, l\, I_f\, K_f) \\
&\quad \times \sum_{m'} (I_f\, l\, M_i - m'\, m' | I_f\, l\, I_i\, M_i) \left(\frac{2I_f+1}{8\pi^2}\right)^{\frac{1}{2}} D^{I_f}_{M_i-m',K_f}(\Theta_i)\, Y_{l,m'}(\theta,\varphi)
\end{aligned} \tag{10}$$

In the above, well-known properties[10] of Clebsch-Gordan coefficients under interchange of indices were employed. From (2) and (3), we can immediately see that

$$\Upsilon^{I_i M_i}_{K_f l\, m;\tau} = \sum_{I_f} (-)^{m+I_f-I_i} (I_i\, l\, K_f+m\, -m | I_i\, l\, I_f\, K_f)\, \Phi^{I_i M_i}_{I_f K_f l;\tau} \tag{11}$$

and hence from (2) that $\Upsilon^{I_i M_i}_{K_f l\, m;\tau}$ has the proper transformation properties and generally contains a mixture of rotational states of the daughter nucleus.

To obtain the differential equations for $w_{\ell,m}(r)$ we substitute (6) in the complete Schrödinger equation, multiply by $\Upsilon^{I_i M_i *}_{K_f \ell' m';\tau}$ and integrate over all the independent variables except r. We get

$$\left[\frac{d^2}{dr^2} + \frac{2\mu}{\hbar^2}(E - E_{\tau,K_f}) - \frac{\ell'(\ell'+1)}{r^2} - \frac{4\mu Ze^2}{\hbar^2 r}\right] w_{\ell',m'}(r) \tag{12}$$

$$- \frac{2\mu}{\hbar^2}\sum_{\ell,m} w_{\ell,m}(r)\,(\ell',m'|H_{rot.}|\ell,m) - \frac{2\mu}{\hbar^2}\sum_{\ell,m} w_{\ell,m}(r)\left(\ell',m'\left|V - \frac{2Ze^2}{r}\right|\ell,m\right) = 0$$

where E_{τ, K_f} merely determines the arbitrary zero of energy. Since the states in general contain more than one member of a nuclear rotational band, the nuclear rotational energy operator is not necessarily diagonal in the Υ representation. The matrix elements of $H_{rot.}$ may be readily evaluated with the aid of the expansion (11) and the relationship

$$H_{rot.}\,\Phi^{I_i M_i}_{I_f K_f \ell;\tau} = \frac{\hbar^2}{2\Im} I_f(I_f+1)\,\Phi^{I_i M_i}_{I_f K_f \ell;\tau}$$

that is,

$$(\ell',m'|H_{rot}|\ell,m) = \frac{\hbar^2}{2\Im}\delta_{\ell\ell'}\sum_{I_f}(-)^{m'-m} I_f(I_f+1) \times (I_i \ell' K_f + m' - m'|I_i \ell' I_f K_f)(I_i \ell' K_f + m - m|I_i \ell' I_f K_f) \tag{13}$$

The electrostatic interaction experienced by the alpha particle, though rather complicated in the space-fixed system, is in the body-fixed system merely the charge on the alpha particle times the electrostatic field of the stationary deformed nucleus. If we make the usual multipole expansion, V is given by

$$V = (2Ze^2/r) + \frac{2e^2 Q_o P_2(\cos\theta')}{2r^3} + \ldots$$

where Q_o is the intrinsic quadrupole moment of the nucleus (the quadrupole moment with respect to the nuclear symmetry axis). With the relation

$$\int Y^{*}_{\ell',m}(\theta,\varphi)\, P_k(\cos\theta)\, Y_{\ell,m}(\theta,\varphi)\, d\omega = C^{(k)}(\ell\, m\,|\,\ell' m) \tag{14}$$

where the $C^{(k)}(\ell m|\ell' m)$ are defined and tabulated by Condon and Shortley,[12] the matrix elements of electrostatic energy can be readily evaluated.

Equation (12) then becomes

$$\left[\frac{d^2}{dr^2} + \frac{2\mu}{\hbar^2}\left(E - E_{T,K_f} - \frac{2Ze^2}{r}\right) - \frac{\ell(\ell+1)}{r^2}\right] w_{\ell,m}(r)$$
$$- \frac{\mu}{\Im}\sum_{I_f,m'} w_{\ell,m'}(r)\,(-)^{m-m'} I_f(I_f+1)\,(I_i\,\ell\, K_f+m'\,-m'\,|\,I_i\,\ell\, I_f K_f)(I_i\,\ell\, K_f+m\,-m\,|\,I_i\,\ell\, I_f K_f) \tag{15}$$
$$- \frac{2\mu}{\hbar^2}\frac{Q_0 e^2}{r^3}\sum_{\ell'} w_{\ell',m}(r)\, C^{(2)}(\ell\, m\,|\,\ell' m) = 0$$

For even-even type alpha emitters, where $I_i = K_f = 0$, equation (15) reduces to a form derived earlier[8, 13]

$$\left[\frac{d^2}{dr^2} + \frac{2\mu}{\hbar^2}\left(E - E_{T,K_f} - \frac{2Ze^2}{r}\right) - \left(\frac{\mu}{\Im} + \frac{1}{r^2}\right)\ell(\ell+1)\right] w_\ell(r) \tag{16}$$
$$- \frac{2\mu}{\hbar^2}\frac{Q_0 e^2}{r^3}\sum_{\ell'} w_{\ell'}(r)\, C^{(2)}(\ell\, 0\,|\,\ell' 0) = 0$$

We now return to the question of the approximate conservation of angular momentum about the symmetry axis and the related question of the axial symmetry of the alpha distribution. As mentioned above, the distribution of alpha particles on the nuclear surface is axially symmetric; that is, on the surface $W_{\ell,\Delta K} \neq 0$ only where $\Delta K = K_i - K_f$. It is to be noted from (15) that the electrostatic potential has no off-diagonal elements in m. The only mixing in of components with $m \neq \Delta K$ results from $H_{rot.}$. This mixing is probably small in the region of large nuclear deformation. Such coupling is in effect ignored by Bohr, Frӧman, and Mottelson[14] when they relate the rotational alpha group intensities between odd and even-even nuclei. The favored alpha decay transitions[14, 15] in which the odd nucleon wave

function remains essentially unaltered are analogous to decay from an even-even nucleus. From this analogy and equation (11) with m = 0 and $K_f = K_i$ (the favored transition) one can obtain for the relative reduced transition probabilities for alpha decay of a given orbital angular momentum to the various possible rotational states

$$B_{\ell I_f} = |(I_i \ell K_i 0 | I_i \ell I_f K_f)|^2 ,$$

which is the relation of Bohr, Fröman, and Mottelson.[14]

THE DECAY EQUATIONS IN SPHEROIDAL COORDINATES

There are two procedures that one could follow in treating alpha decay. In the first, the decay equations are integrated outwards starting with nuclear surface boundary values which may be arrived at by a model describing the formation and behavior of alpha particles in nuclear matter. The other procedure is almost the reverse of the first and consists of starting at infinity with experimental amplitudes and integrating in to the nuclear surface. (It should be noted here that the alpha group intensity measurements do not yield information regarding the relative phases.)

In either approach it is necessary to work with the equations in regions close to the nuclear surface, for there the non-central electrostatic field is most effective in coupling the various partial waves. Since in the following we shall assume that the nuclear surface is a prolate spheroid, it is convenient to use prolate spheroidal coordinates.

We take the foci of the spheroids to be at $(x = y = 0;\ z = \pm a/2)$ and define the spheroidal coordinates of a point in space as

$$\begin{aligned} \xi &= (r_1 + r_2)/a \qquad 1 \leq \xi \leq \infty \\ \eta &= (r_1 - r_2)/a \qquad -1 \leq \eta \leq 1 \\ \phi &= \tan^{-1}(y/x) \qquad 0 \leq \phi \leq 2\pi \end{aligned} \tag{17}$$

where r_1 and r_2 are the distances between the point and the two foci. a is specified by the condition that one of the spheroids, $\xi = \xi_o$, corresponds to the surface of the nuclear spheroid. Asymptotically, the connection to spherical polar coordinates is as below:

$$\begin{aligned} \xi &\longrightarrow (2r/a) \\ \eta &\longrightarrow \cos\theta \\ \phi &= \phi \, . \end{aligned}$$

We shall consider the special case of an even-even ($I_i = 0$) nucleus. The wave equation in spherical coordinates in the coordinate system fixed in the daughter nucleus is, from (16),

$$\left[-\frac{\hbar^2}{2\mu}\Delta - \frac{\hbar^2}{2\Im} L(\theta,\phi) + V(r,\theta) - E\right]\psi = 0 \tag{18}$$

where

$$L(\theta,\phi) = r^2\left[\Delta - \frac{1}{r^2}\frac{\partial}{\partial r}\left(r^2\frac{\partial}{\partial r}\right)\right]$$

Since the lowest band of an even-even nucleus is characterized by K = 0, and since we are considering only decay to the lowest band, the alpha particle wave function will be axially symmetric ($M = K_i - K_f = 0$). In prolate spheroidal coordinates, (18) becomes for axially symmetric wave functions,

$$\left\{\frac{4}{a^2(\xi^2-\eta^2)}\left[\frac{\partial}{\partial\xi}(\xi^2-1)\frac{\partial}{\partial\xi} + \frac{\partial}{\partial\eta}(1-\eta^2)\frac{\partial}{\partial\eta}\right] + \frac{\mu}{\Im}\frac{(\xi^2-1)}{(\xi^2-\eta^2)}\frac{\partial}{\partial\eta}(1-\eta^2)\frac{\partial}{\partial\eta}\right. \tag{19}$$
$$\left. + \frac{2\mu}{\hbar^2}(E - V(\xi,\eta))\right\}\psi(\xi,\eta) = 0$$

The rotational energy term is not exactly represented by the second term in (19). This term is an approximation good when $\xi^2 >> \eta^2$. For the deformations

expected in actual nuclei the condition is not fulfilled near the surface ($\xi_o = 1.5$ for Pu^{238}), but near the surface the whole rotational term is negligible compared with the potential energy. When the term becomes important (near and beyond the turning point), the approximate expression is accurate.

If we represent the wave function by the expansion

$$\psi(\xi,\eta) = \sum_{\ell} (\xi^2-1)^{-\frac{1}{2}} w_\ell(\xi)\, Y_{\ell,0}(\cos^{-1}\eta, \varphi) \tag{20}$$

we obtain for the equation satisfied by $w_\ell(\xi)$

$$\frac{d^2 w_\ell}{d\xi^2} + \left[\frac{1}{(\xi^2-1)^2} - \ell(\ell+1)\left(\frac{1}{\xi^2-1} + \frac{\mu a^2}{4\xi}\right)\right] w_\ell(\xi) + \frac{\mu a^2}{2\hbar^2(\xi^2-1)} \sum_{\ell'} w_{\ell'}(\xi) \int Y^*_{\ell,0}\left[E - V(\xi,\eta)\right](\xi^2-\eta^2) Y_{\ell',0}\, d\xi\, d\eta = 0 \tag{21}$$

We wish now to obtain the potential $V(\xi, \eta)$ with the assumption that the charge density is uniform throughout the nuclear spheroid. This can easily be accomplished by integrating the Green's function for Laplace's equation in spheroidal coordinates[16] over the nuclear volume; and we find

$$V(\xi, \eta) = \frac{4Ze^2}{a}\left(Q_o(\xi) - P_2(\eta)Q_2(\xi)\right) \tag{22}$$

where $Q_o(\xi)$ and $Q_2(\xi)$ are Legendre functions of the second kind and equal to

$$Q_o(\xi) = \frac{1}{2}\ln\frac{(\xi+1)}{(\xi-1)}$$

$$Q_2(\xi) = P_2(\xi)\frac{1}{2}\ln\frac{(\xi+1)}{(\xi-1)} - \frac{3}{2}\xi$$

Asymptotically, $V(\xi, \eta)$ can be expressed in spherical coordinates as

$$V(\xi, \eta) \longrightarrow \frac{2Ze^2}{r} + \frac{Q_o e^2 P_2(\cos\theta)}{r^3} + \ldots \tag{23}$$

where $Q_o = \frac{Za^2}{10}$.

The above relationship between the intrinsic quadrupole moment, Q_o, and the interfocal distance, a, permits us to determine a from experimental data.

Evaluating the integral in (21) by using (14) and

$$\int Y^*_{l',0}(\eta)\, P_2(\eta)\, \eta^2\, Y_{l,0}(\eta)\, d\omega = \frac{12}{35} C^{(4)}(l0;l'0) + \frac{11}{21} C^{(2)}(l0;l'0) + \frac{2}{15}\delta_{ll'} \tag{24}$$

we obtain for the Schrödinger equation in the exterior region.

$$\frac{d^2}{d\xi^2} w_l - (V_0 + V_l)\, w_l - \sum_{l'} w_{l'} (V^{(2)}_{ll'} + V^{(4)}_{ll'}) = 0$$

where

$$\begin{aligned}
V_0(\xi) &= \frac{2\mu Z e^2}{\hbar^2(\xi^2-1)}\left(\xi^2 - \frac{1}{3}\right)\left[Q_0(\xi) - \frac{E a}{4Ze^2} + \frac{2}{15} Q_2(\xi)\right] - \frac{1}{(\xi^2-1)^2} \\
V_l(\xi) &= l(l+1)\left(\frac{1}{\xi^2-1} + \frac{\mu a^2}{4\mathfrak{I}}\right) \qquad (25) \\
V^{(2)}_{ll'}(\xi) &= \frac{2\mu Z e^2 a}{\hbar^2(\xi^2-1)}\, C^{(2)}(l0;l'0)\left[\frac{2}{3} Q_0(\xi) - \frac{Ea}{4Ze^2} + \left(\xi^2 - \frac{11}{21}\right) Q_2(\xi)\right] \\
V^{(4)}_{ll'}(\xi) &= \frac{2\mu Z e^2 a}{\hbar^2(\xi^2-1)}\, \frac{12}{35}\, C^{(4)}(l0;l'0)\, Q_2(\xi)
\end{aligned}$$

The coupling between various L-waves results in part from the non-central nature of the field and in part from the nature of the spheroidal coordinate system. The Coulomb term is contained in V_0, and $V^{(2)}_{ll'}$ is significantly larger than $V^{(4)}_{ll'}$ throughout the region of interest.

GENERAL PROCEDURE IN NUMERICAL WORK

In all of the regions that must be considered in the treatment of decay through a single barrier (the "barrier" region, the "turning-point" region, and the "far" region) the calculations for the present problem are obviously more

difficult than for the corresponding problem with uncoupled waves. However, since the coupling decreases rapidly with distance, we need only give special consideration to the barrier and turning-point regions (the wave functions being very nearly Coulombic in the far region).[17]

In the following we shall seek approximate solutions to

$$\begin{aligned} w_o'' - V_o w_o &= V_{o2} w_{o2} + V_{o4} w_4 \\ w_2'' - (V_o + V_2) w_2 &= V_{o2} w_o + V_{24} w_4 \\ w_4'' - (V_o + V_4) w_4 &= V_{o4} w_o + V_{24} w_2 \end{aligned} \tag{26}$$

which is the set of equations (25) in which all of the partial waves with $L > 4$ are neglected.

Within the barrier region the wave functions undergo extremely large variations in their magnitudes, making direct calculations with (26) difficult. Instead we have preferred to work with the ratios $y(\xi) = w_2/w_o$ and $z(\xi) = w_4/w_o$ inasmuch as their magnitudes vary within a small range. Solutions for $y(\xi)$ and $z(\xi)$ arising from a WKB-type approximation are

$$y(\xi) = [(K_o)/(K_2)]^{1/2} \exp\{-\int (K_2 - K_o) d\xi\}$$

$$z(\xi) = [(K_o)/(K_4)]^{1/2} \exp\{-\int (K_4 - K_o) d\xi\}$$

where

$$\begin{aligned} K_o &= [V_o + V_{o2} y + V_{o4} z]^{1/2} \\ K_2 &= [V_o + V_2 + V_{o2}/y + (z/y) V_{24}]^{1/2} \\ K_4 &= [V_o + V_4 + (1/z) V_{o4} + (y/z) V_{24}]^{1/2} \end{aligned} \tag{27}$$

As a result of the coupling the equations (27) themselves constituted an extremely complicated set of integral equations. We have solved (27) by an iterative procedure in which $y(\xi)$ and $z(\xi)$ are assumed over a small range of ξ

and are used to calculate improved y's and z's.

This procedure, which was continued until self-consistent values were obtained, was found to converge fairly rapidly. To circumvent the difficulty occurring where y or z goes through zero a change of dependent variable of the type $\bar{y} = (w_2 + bw_o)w_o^{-1} = y + b$ with b a constant, was made. Barrier region integrations were made in this manner for both outward and inward integrations.

The solutions (27) are, of course, inapplicable in the turning point region. In this region the wave functions do not vary radically, so that it is feasible to work with the wave equations directly in the form of (26).

Outward Integrations for Cm^{242}.--It was decided at first to see if the simpler pictures of the alpha particle in nuclear matter could lead to the observed ratio of the partial waves. Cm^{242} was selected as an interesting case, as it exhibits a very large L = 4 hindrance factor. Probably the simplest models are the one-body model in which the alpha particle is thought to move intact in nuclear matter for at least a few traversals of the nucleus and the model in which alpha particles are formed uniformly on the surface of the nucleus. The angular distribution with reference to the nuclear symmetry axis is then altered by the non-uniform barrier.

For the individual alpha particle model we assume that the alpha particle is in the lowest state in a spheroidal well (of uniform depth) the depth of which is adjusted so that the emitted alpha particle has the experimentally observed energy. The wave equation for the interior region is separable in spheroidal coordinates and has as its solution an "angular" part which may be expressed as an infinite sum of Legendre polynomials in η and a "radial" part which is a sum of spherical Bessel functions in ξ.[16] From these solutions the boundary

values of the alpha particle wave function on the nuclear spheroid are obtained.

It is appropriate at this point to look into the questions of the size (in this context, the volume) and the shape (i.e., the interfocal distance) of the nuclear spheroid. There is some uncertainty regarding the appropriate nuclear size[18] to be used in these considerations. Thus, our calculations were performed for two "sizes" of nuclei. One had a volume equal to that of a sphere of radius $1.20\ A^{1/3} \times 10^{-13}$ cm., the other to a sphere of radius $1.35\ A^{1/3} \times 10^{-13}$ cm.

To determine the interfocal distance, a, of the nuclear spheroid (hence of the spheroidal coordinate system employed) use was made of the relation (23) between Q_o and a. Since the intrinsic quadrupole moment for Pu^{238} is not empirically known, we used a semiempirical connection[8] between quadrupole moments and energy of the first rotational state, E_2(kev):

$$|Q_o| = 1.2Z \times E_2^{-1/2} \times 10^{-24}\ \text{cm}^2$$

where Z is the charge. This formula is based on the experimentally known relation between intrinsic quadrupole moments (from gamma ray lifetimes and Coulomb excitation cross sections) in the heavy rare earth region. The formula yields a $|Q_o|$ of 17×10^{-24} cm^2 for Pu^{238}. Subsequent to the completion of our calculations the values of $|Q_o|$ for U^{238} and Th^{232} of 8×10^{-24} cm^2 and 9×10^{-24} cm^2, respectively, were determined by Temmer and Heydenburg[19] on the basis of Coulomb excitation cross sections. It thus appears that the relation (28) may overestimate the intrinsic quadrupole moment by as much as 50 percent and that we have used a somewhat too large value of $|Q_o|$ for our calculations. In view of this, the quantitative details of our numerical work are subject to considerable modification, but it seems likely that none of our major qualitative conclusions will be altered.

The assumption of uniform charge density may be open to question in that it is expected that the protons beyond the closed shell of 82 will fill the lower energy orbitals with maximum concentration in the ends of the prolate spheroid. There is insufficient knowledge to justify any such refinement here.

The interfocal distance, a, corresponding to Q_o being used for Pu^{238} is 1.35×10^{-12} cm. With this value of a, the two nuclear surfaces are prolate spheroids defined by the coordinate surfaces $\xi_o = 1.41$ and $\xi_o = 1.51$.

Table I summarizes the results of these calculations. It is seen that there is some suppression of the L = 4 group, but the agreement with the experimental intensities is not satisfactory. We can only conclude that neither simple picture represents the physical situation.

Dresner[13] has independently drawn the same conclusion from his work.

Table I

Results of Outward Integrations for Cm^{242}

	ξ_o	Boundary conditions at ξ_o		Calculated values at $\xi = 5.6$		Calculated α group intensity (using connection formula approximation)	
		y_o	z_o	y	z	$a_2:a_o$	$a_4:a_o$
uniform surface	1.406	0	0	+1.20	+0.298	1.13	0.058
distribution	1.514	0	0	+0.91	+0.230	0.68	0.035
one-body model	1.406	-0.277	+0.025	+0.83	+0.202	0.56	0.029
	1.514	-0.232	+0.016	+0.72	+0.156	0.43	0.017
values needed to match experimental intensities				+0.74	-0.02	0.357	4.8×10^{-4}

Inward Integrations for Cm^{242} and Th^{228}.--As mentioned earlier, one can exploit the available experimental data directly by integrating the equations for the various partial waves inwards to the nuclear surface and thus obtain information about the alpha probability distribution on the nuclear surface. In the following we shall restrict ourselves to the study of the two nuclides Cm^{242} and Th^{228}. These nuclides are of interest in that they exhibit opposite extremes in the L = 4 hindrance factors, Cm^{242} being very strongly hindered and Th^{228} being virtually unhindered. The data and information pertinent to our calculations on these two nuclides are presented in Table II.

Table II

Information Used in Inward Integration Studies

Nucleus	Alpha disintegration energy (including electron screening)(Mev)	Energy of 2+ state (Mev)	Energy of 4+ state (Mev)	Relative alpha abundance to 0^+	2^+	4^+	Assumed Q_0 of daughter (10^{-24} cm^2)
Cm^{242}	6.252	0.044	0.146	73.7	26.3	0.035	+17
Th^{228}	5.553	0.084	0.253	71	28	0.2	+11.6

The observed intensities, of course, determine only the amplitudes of the various L waves but not their phases. The condition used to determine the possible sets of phases was that the phase factors, $e^{i\delta_\ell}$, of the waves, which are pure outgoing waves at large separations, be such as to produce an exponential damping of the imaginary part of the partial waves within the barrier. With these phases one can then obtain the real part of the wave by inward integration.

In carrying out the above procedure of integrating through the turning point and into the barrier region we have used two different methods. The first, which is simple but very approximate, is based on the circumstances that the equations (26) are decoupled at the turning point in that prolate spheroidal coordinate system in which the interfocal distance $\underline{a}$, is given by $\underline{a}^2 = 6Q_o/Z$. Assuming that the coupling terms remain negligible (compared to the remaining terms in the equation) in a small region about the turning point (an assumption probably reasonable for the Th^{228} case) one can apply the simple WKB connection prescription. A transformation to the spheroidal coordinate system appropriate for the barrier region of the nucleus in question is then performed.

It is important to note that the phase determination procedure yields not one but four sets of relative phases for the three partial waves. This is most readily seen when the coupling can be neglected, as in the above-mentioned approximation. If δ_ℓ insures that the part increasing exponentially as $\xi \to 1$ is pure real, so will $\delta_\ell + \pi$.

Due to the very small magnitude of w_4 as compared to w_2 and w_o in the case of Cm^{242} the assumption of negligible coupling in the turning point region in the special coordinate system is not valid. In this case we resorted to direct numerical solutions to equations (26) (in spherical coordinates) on the UCRL Bush-type electromechanical differential analyzer.[20]

Table III summarizes the results for the integrations through the turning point. The values of $y(\xi_1)$ and $z(\xi_1)$ contained therein served as initial values for the integrations in the barrier region by the method described in the preceding section. There are two additional phase choices for Cm^{242} which because of the small magnitude of w_4 in the turning point region lead to essentially the same results as the two listed sets.

Table III

Initial Values for the Barrier Integrations

	Cm^{242} ($\xi_1 = 5.6$)		Th^{228} ($\xi_1 = 6.0$)			
	Case I	Case II	Case I	Case II	Case III	Case IV
$y(\xi_1)$	0.74	-0.77	0.93	0.94	-0.94	-0.93
$z(\xi_1)$	-0.022	0.025	0.18	-0.23	0.22	-0.17

While the several sets of $y(\xi_1)$ and $z(\xi_1)$ values lead to the observed intensity and proper behavior of the imaginary part, all but one for each nucleus are physically unlikely. Unless the distribution of alpha particles on the nuclear surface is restricted to a narrow band about the equator, we would expect that in the turning point region the distribution will be at least somewhat peaked at the poles because of the lower barrier in those directions. On the basis of these considerations we can select the physically most plausible set, and in Figs. 2 and 3 are shown the results of the integrations for these cases in the two nuclei. (Cases I)

The other choices of phases listed in Table III were also studied. Case II for Th^{228} exhibits a somewhat pathological behavior in that y and z increase drastically in the integration inwards. Thus, this choice of phases is unlikely to represent the physical situation.

In Fig. 4 we have plotted the surface distributions for all the above cases. It is to be noted that the $|\psi|^2_{\text{surface}}$ are symmetric about the equator, since only even L values enter in the decay to the lowest band of an even-even nucleus. In each case the distributions are given for the two sizes of nuclei. The results do not differ much with the variation in volume considered here.

As expected, all but the two physically probable sets of initial values at ξ_1 lead to $|\psi|^2_{surface}$ narrowly restricted about the equator of the spheroids. Granting that cases I probably represent the physically significant cases for both Th^{228} and Cm^{242} we can observe that there is a shift in the surface distribution from a broad peak about the poles in Th^{228} to one more concentrated in the regions midway between poles and the equator in the case of Cm^{242}. That the shift in surface distribution is gradual can be inferred from the continuous growth of the hindrance factor in going from Th^{228} to Cm^{242}. (Cf. Fig. 1.)

It was suggested in a preliminary report[8] on the coupled alpha decay problem that for nuclei of greater atomic number and deformation than Cm^{242} the continuation of the intensity trend might show a reversal of the decreasing behavior of the L = 4 group. The increasing L = 4 group of these heaviest nuclei would bear a phase relationship with respect to the L = 0 group which was the opposite of that of the lower mass alpha emitters. Subsequent to this speculation the study[3] of alpha emitters Cf^{246} and Fm^{254} actually showed the increase in abundance of the L = 4 group. The discussion of the preliminary report[8] also suggested speculatively that the intensity of the L = 2 group might begin to decrease for heavier nuclei, and this also was found subsequently for californium and fermium isotopes. The idealized model on which these guesses were based considered a sharp angular alpha distribution of a delta function nature. The qualitative success of the guesses certainly does not imply any detailed validity of the delta function picture. Indeed, it seems most probable that the alpha angular distributions, particularly in the turning point region, are fairly broad. Our numerical results cannot really answer the question, as we have not included higher partial waves than L = 4, but the hindrance factors for higher groups are uniformly very large. The

more groups that are included in the integrations, the more detailed can be the information on the alpha distribution at the nuclear surface. Sharply peaked functions are unlikely due to the high rotational kinetic energy associated with them.

Total Barrier Penetration.--It is of interest to see how the occurrence of a spheroidal deformation affects the total decay constant. Let us define a generalized penetration factor P as

$$P = \frac{\int_{S_\infty} |\psi|^2 dS}{\int_{S_n} |\psi|^2 dS}$$

where S_∞ is a surface at a large distance from the nucleus and S_n is the nuclear surface. ψ is the complete wave function, which asymptotically goes over into a pure outgoing wave. For the case of a spherical nucleus the penetration factor obtained using first order WKB wave functions is

$$P_C = [E/(V(R)_n - E)]^{1/2} \exp\{-(2/\hbar)\int_{R_n}^{R_{T.P.}} \sqrt{2m(V(r)-E)}\, dr\}$$

where R_n is the nuclear radius and $R_{T.P.}$ is the classical turning point.

With y and z known as functions of ξ, it is a simple matter to compute the penetrability for the spheroids taken in the above calculations. Table IV represents the results of the penetration factor calculations for the Th^{228} and Cm^{242} with the nuclear volumes in all cases equal to those for spherical nuclei with radii $R = 1.20 \times 10^{-13} A^{1/3}$ cm. The inward integration results, Cases I, are used.

In the last column of Table IV are the values predicted by the Hill-Wheeler[7] one-dimensional WKB formula for penetration factor, evaluated

through the thinnest part of the barrier. While both the Hill-Wheeler formula and the present work lead to larger penetrabilities than in the case of the spherical nucleus (as would be expected), the one-dimensional formula predicts a much larger increase than the detailed treatment and a much larger increase for Cm^{242} than for Th^{228}. This last fact is rather difficult to reconcile with the success of the old correlations of decay rate data with spherical barrier formulas. The much lower enhancement of penetrability which the present numerical work finds does much to remove the above difficulty.

Table IV

Barrier Penetration Factors

Alpha emitter	Ln P_C (spherical)	Ln P_{DI} (spheroidal case I) (this work)	Ln(P_{DI}/P_C) (this work)	Ln (P_D/P_C) Hill-Wheeler 1-dimensional WKB formula
Th^{228}	-74.73	-72.58	2.15	4.98
Cm^{242}	-72.79	-70.39	2.40	6.77

It appears then that the one-dimensional formula does not give a good estimate for the alpha decay problem. The alpha decay process is not able nearly to take full advantage of the much thinner barrier in the vicinity of the poles. The reason for the failure of the one-dimensional estimate may be expressed qualitatively as follows: if the alpha wave function were to be sharply channeled along the most favorable penetration trajectory, the total wave function would contain high angular momenta components with large amplitudes. The increased centrifugal barrier and higher nuclear rotational

energy associated with the wave function would produce a dissipation of the wave function along the trajectory much larger than the one-dimensional WKB integral indicates. The wave function adjusts itself to a compromise involving moderate angular concentration of the wave function along the favorable penetration trajectory.

One can also note from Column 3 of Table IV that the spheroidal shape enhances the penetration factor of Th^{228} almost as much as that of Cm^{242} despite the fact that Cm^{242} has appreciably larger deformation. This is easily understood when we consider that the distribution of alpha particles on the nuclear surface is peaked about the axis in the case of the Th^{228} while the peak for the Cm^{242} is closer to the equator.

CONCLUSIONS

From the numerical work we are able to gain some information on alpha particle formation in nuclear matter. Both from failure of the one-body model to yield the proper ratio of intensities in the Cm^{242} case and from the shift of the peaks of the surface density with mass, we can conclude that the one-body model does not adequately represent the physical situation. That is, the alpha particle has a transitory existence in the nucleus and it does not move intact for times of the order of a period. We must envision the alpha clusters as continually forming and dissolving with short mean free paths.

Also the picture of alpha particles being distributed uniformly on the nuclear surface does not appear to represent the physical state of affairs.

We might think of the situation in the following way: the alpha clusters that have any appreciable probability of forming and penetrating the barrier are those which are made up of the most loosely bound neutrons and protons.

The distribution of these clusters will then reflect the distribution of the most loosely bound nucleons. If, as we expect, case I is the one that corresponds to the correct picture, we would conclude that the outer nucleons tend to concentrate near the poles in Th^{228} and nearer to the equator in Cm^{242}. In a prolate spheroidal well of appreciable eccentricity, the states concentrated near the poles are expected to be filled first.[21] These are the states with Bohr-Mottelson quantum numbers $\Omega = \pm 1/2$ (all other states have nodes at the poles). One might suppose that orbitals with large probability densities at the poles are filled around A = 230 and that subsequent nucleon pairs tend to fill states with density distributions shifted toward the equator.

ACKNOWLEDGMENT

We wish to acknowledge the valuable assistance of Dr. John Killeen in adapting the appropriate part of the numerical work for the differential analyzer, and of Mr. Victor Brady and others of the differential analyzer team for the execution of the work. We are grateful to Mrs. Bonnie Gronlund and Mrs. Harriet Reardon for their assistance in much computational work. We wish to thank Professor I. Perlman and Dr. Frank Asaro for generously making available much experimental data in advance of publication. We have enjoyed interesting discussions with Dr. A. Bohr, Dr. B. R. Mottelson, Professor R. F. Christy, and Professor J. A. Wheeler.

This work was performed under the auspices of the U. S. Atomic Energy Commission.

REFERENCES

1. For a review of the experimental data and for an extensive list of references see:

A. Bohr, Rotational States of Atomic Nuclei, Ejnar Munksgaard, Copenhagen (1954) and A. Bohr and B. R. Mottelson, Chapter 17 of Beta and Gamma Ray Spectroscopy, edited by K. Siegbahn, North-Holland Publishing Company, Amsterdam (1955).

2. A. Bohr, Dan. Mat. Fys. Medd. 26, No. 14 (1952); A. Bohr and B. R. Mottelson, Dan. Mat. Fys. Medd. 27, No. 16 (1953).

3. I. Perlman and F. Asaro, "Alpha Radioactivity," Ann. Rev. Nuclear Science 4, 157 (1954) (Stanford, California).

4. F. Asaro, unpublished (1955).

5. M. A. Preston, Phys. Rev. 71, 865 (1947).

6. It is of interest to compare the hindrance factors for alpha particles having angular momentum $L \geq 4$ to the reduction expected from the centrifugal barrier. Thomas (ref. a) for example, has calculated the reduction factors, η_ℓ, in the JWKB approximation and finds that for a 5-Mev uranium alpha emitter they are 0.59 for L = 2 and 0.18 for L = 4. The smaller results of Devaney (ref. b) appear to be in error. From the approximate formulas of Gamow and Critchfield, (ref. c) one can obtain the following simple expression for η_ℓ, which agrees fairly well with Thomas's results:

---

a. R. G. Thomas, Prog. of Theor. Phys. 12, 253 (1954).

b. J. J. Devaney, Phys. Rev. 91, 587 (1953).

c. G. Gamow and C. L. Critchfield, Theory of Atomic Nucleus and Nuclear-Energy Sources, Oxford (1949), p. 173.

$$\eta_{\ell} = \exp\left[- \frac{\hbar\ell(\ell+1)}{(MR)^{1/2}(Z-2)^{1/2}e} \right]$$

where Z is the atomic number, R the effective nuclear radius, and M the mass of the alpha particle. From the above, it is evident that nowhere in the alpha emitter region will η_{ℓ} be small enough to account for the observed $L \geq 4$ hindrance factors.

7. D. L. Hill and J. A. Wheeler, Phys. Rev. 89, 1102 (1953); p. 1134.

8. J. O. Rasmussen, University of California Radiation Laboratory Unclassified Report UCRL-2431 (1953), unpublished.

9. M. A. Preston, Phys. Rev. 75, 90 (1949).

10. Cf. E. U. Condon and G. H. Shortley, The Theory of Atomic Spectra, Cambridge (1935).

11. B. Segall, Phys. Rev. 95, 605A (1954).

12. E. U. Condon and G. H. Shortley, loc. cit., 175 ff.

13. L. Dresner, Ph. D. Thesis, Princeton University, 1955 (unpublished).

14. A. Bohr, P. O. Fröman, and B. R. Mottelson, Dan. Mat. Fys. Medd. 29, No. 10 (1955).

15. J. O. Rasmussen, Arkiv för Fysik 7, 185 (1953).

16. P. M. Morse and H. Feshbach, Methods of Theoretical Physics, McGraw-Hill (1953), Part II, p. 1291.

17. R. F. Christy, Phys. Rev. 98, 1205A (1955); and L. Dresner and J. A. Wheeler (ref. 13) have also studied the problem of decay through a nonspherical barrier.

18. On the assumption of spherical shape various nuclear radii have been obtained by different experiments. For example, the Stanford high

energy electron scattering data (ref. d) yield what might be called a charge radius of $1.1\ A^{1/3} \times 10^{-13}$ cm. This value is probably small for our purpose, as it neglects the greater extension of the neutrons (ref. e) the finite range of nuclear forces, and the radius of the alpha particle. The radius of the alpha particle is about 2×10^{-13} cm as determined by electron scattering. The alpha particle scattering measurements of Farwell and Wegner (ref. f) indicate a value of $(1.50\ A^{1/3} + 1.4)\ 10^{-13}$ cm, but this is probably more a measure of the major axis of the spheroid (because of the lower barrier at the tips) and hence a large value for the spherical shape. See also Tolhoek and Brussard (ref. g), regarding effective radii for alpha decay.

19. G. M. Temmer, private communication (1955).

20. J. Killeen, University of California Radiation Laboratory Report UCRL-2239 (1953).

21. L. Dresner and J. A. Wheeler have explored this aspect of the problem independently (ref. 13).

---

d. D. R. Yennie, D. G. Ravenhall, and R. N. Wilson, Phys. Rev. 95, 500 (1954).

e. M. H. Johnson and E. Teller, Phys. Rev. 93, 357 (1954).

f. Farwell and Wegner, Phys. Rev. 95, 1212 (1954).

g. H. A. Tolhoek and P. J. Brussard, Physica 21, 449 (1955).

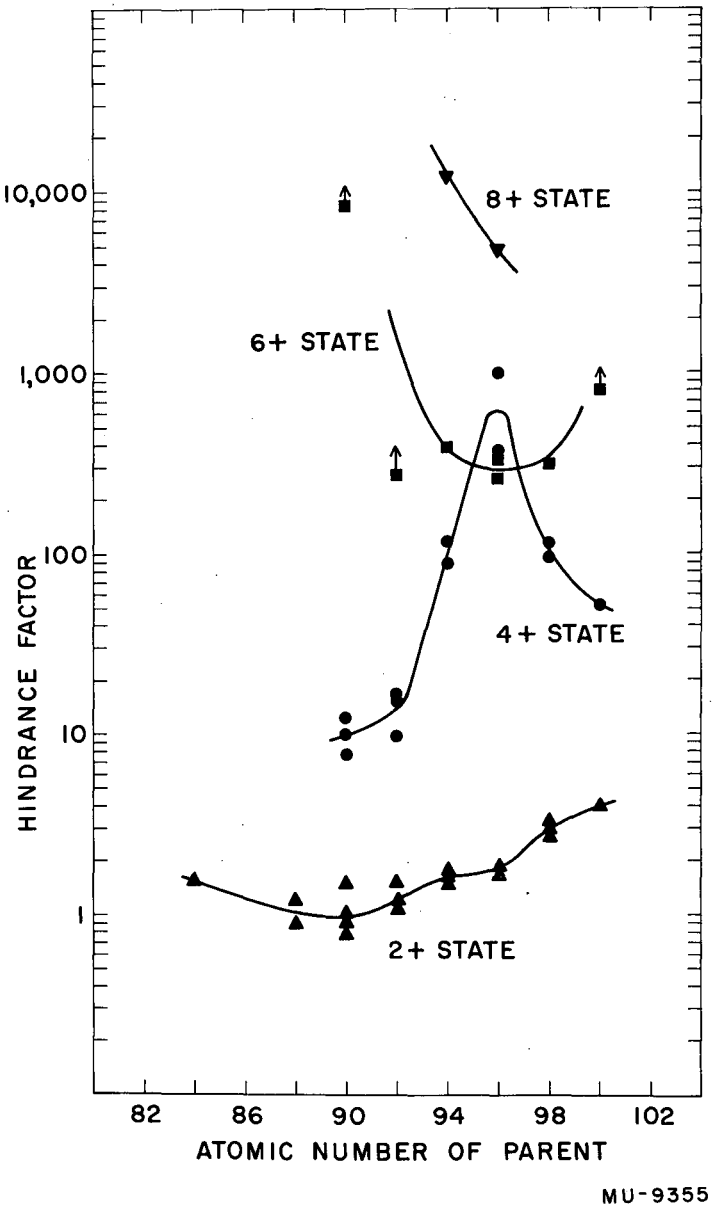

Fig. 1. Hindrance factors of alpha groups in even-even nuclei (defining the ground-state transition as unhindered) from Asaro.[4]

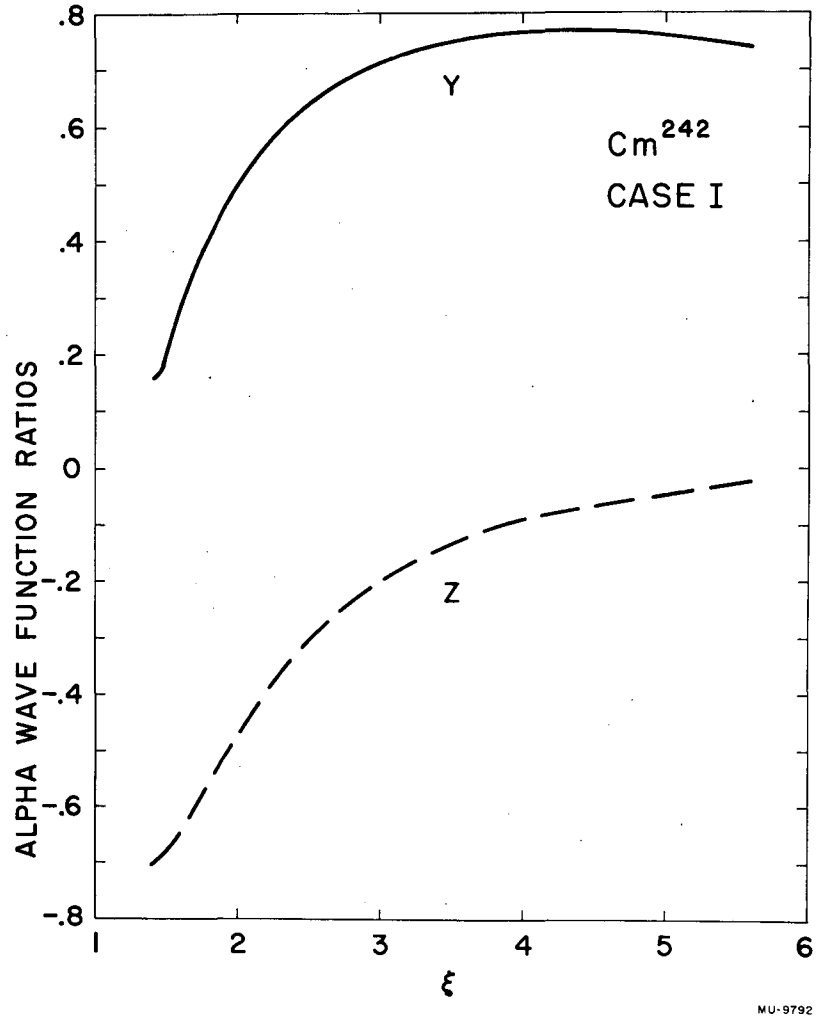

Fig. 2. Results of an inward numerical integration of the alpha wavé equation for Cm^{242} in prolate spheroidal coordinates (Case I). Boundary conditions at $\xi = 5.6$ are based on experimental alpha group intensities. y goes over asymptotically into the ratio of wave amplitudes of $\ell = 2$ and $\ell = 0$ groups, and z, into the ratio of the $\ell = 4$ to the $\ell = 0$ groups.

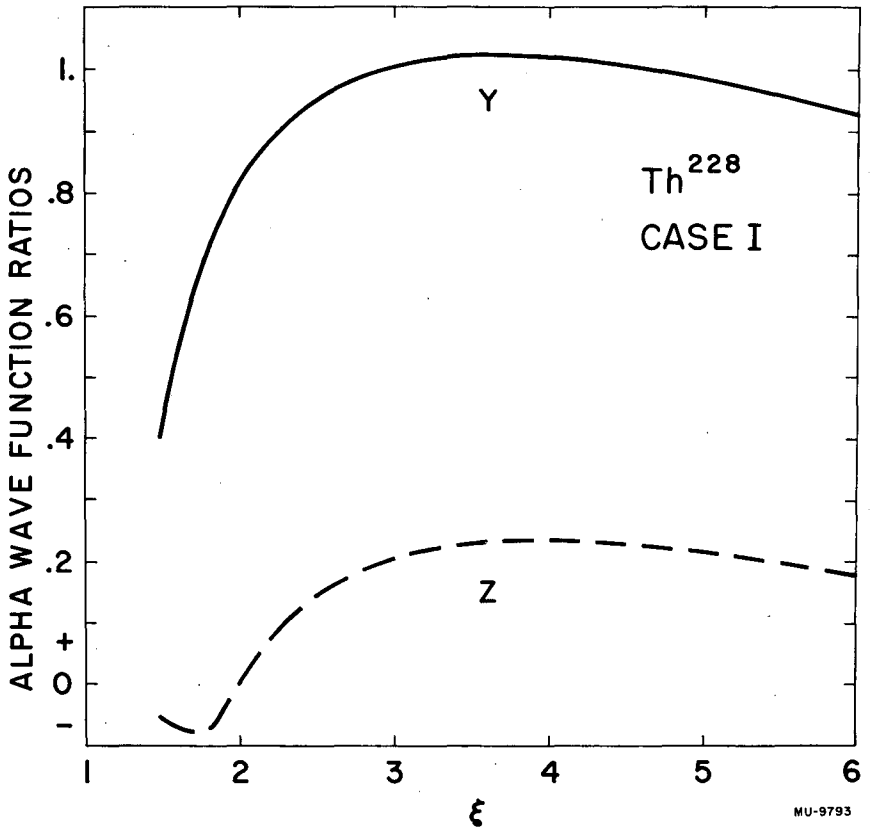

Fig. 3. Results of an inward numerical integration of the alpha wave equation for Th^{228} in prolate spheroidal coordinates (Case I). Boundary conditions at $\xi = 6$ are based on experimental alpha group intensities.

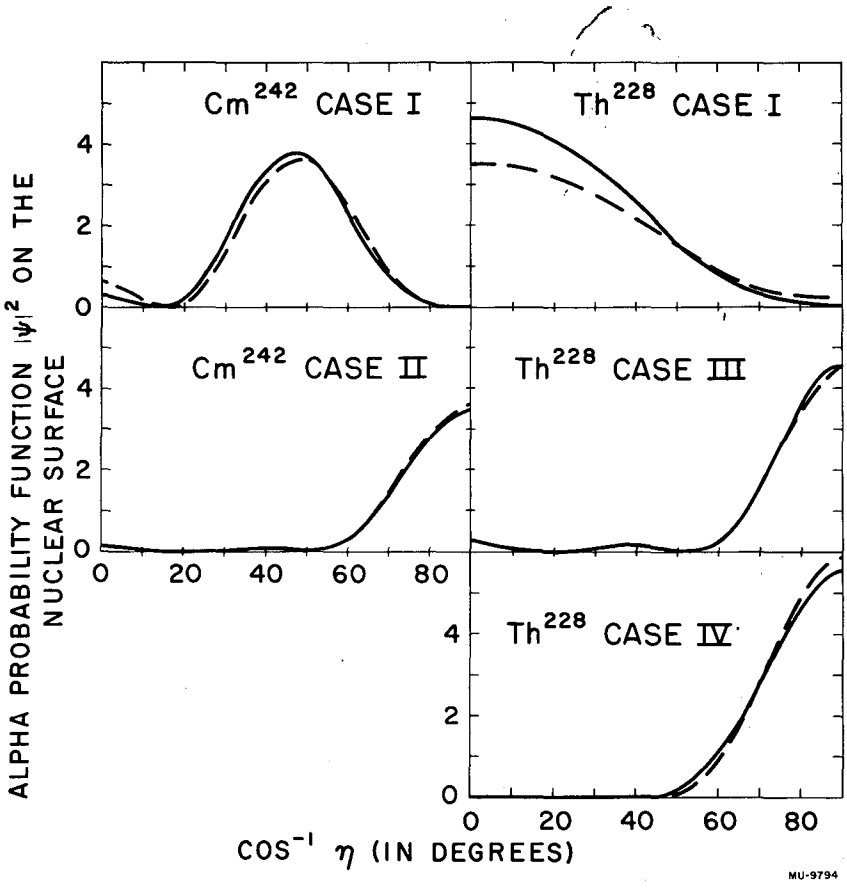

Fig. 4. Calculated alpha probability distributions on the spheroidal nuclear surface from inward integrations based on experimental alpha group intensities. The different cases result from different possible choices of relative phases of the various partial waves. Cases I for Cm^{242} and Th^{228} are believed to be the most likely physically significant cases. The solid lines correspond to choice of the surface to enclose a volume equal to that of a sphere of radius $1.35 \times 10^{-13} A^{1/3}$ cm, and the dashed lines, to radius $1.20 \times 10^{-13} A^{1/3}$ cm.